Design of Low-Density Parity-Check Codes for Multi-Input Multi-Output Channels

Stephan ten Brink, Gerhard Kramer, Alexei Ashikhmin
Bell Labs, Lucent Technologies
600 Mountain Ave, Murray Hill NJ 07974, U.S.A.
e-mail: {stenbrink,gkr,aea}@research.bell-labs.com.

Abstract

A combined coding and modulation scheme is studied for transmitting information reliably over multi-input multi-output (MIMO) fading channels. The scheme, called low-density parity-check (LDPC) modulation, combines the MIMO detector and the variable node decoder of a low-density parity-check (LDPC) code. Good LDPC degree sequences are designed by using extrinsic information transfer (EXIT) charts. LDPC modulation is shown to perform within about 1 dB of MIMO capacity when the receiver, but not the transmitter, knows the channel. The method further outperforms a UMTS standard turbo coding scheme by a wide margin when there are more transmit than receive antennas.

I. Introduction

Iterative decoding of low–density parity–check (LDPC) codes is a powerful method for approaching capacity on noisy channels [1]–[5]. The most important design problem for these codes is finding good degree sequences for the modulation, channel and detector under consideration. We show how to use extrinsic information transfer (EXIT) charts [6] to solve this problem for both the additive white Gaussian noise (AWGN) channel and multi–input, multi–output (MIMO) fading channels [7], [8].

We will consider primarily the case where the channel is known at the receiver but not at the transmitter (see, e.g., [9, pp. 2627–2629]). Previous work has shown that MIMO detectors and turbo codes do not work well together when there are more transmit than receive antennas [10]. We instead study a scheme that combines the MIMO detector with part of the LDPC decoder. A similar technique has been considered by others, e.g. [11], but without attempting to design LDPC degree sequences. We show that the scheme can in fact approach capacity by designing degree sequences that are well matched to the MIMO detector. The combined coding/modulation technique could be called *LDPC modulation*. Other approaches to combining coding and modulation are trellis coded modulation [12], bit–interleaved coded modulation [13]–[19], or space–time block coded modulation [20], [21].

This paper is organized as follows. In Section II we design LDPC codes for the AWGN channel by using EXIT charts. Note that although we focus exclusively on EXIT charts, alternative design tools exist and can be found in [5], [22], [23]. In Section III we describe how one can combine the MIMO detector with the LDPC decoder. Section III further extends the design methodology of Section II to design LDPC modulation schemes that operate close to MIMO capacity. The performance compares favorably with a scheme employing turbo codes.

II. EXIT chart for LDPC Codes on AWGN Channels

The structure of the decoder for a LDPC code of length n and (design) rate $R = k/n$ is as follows. The decoder has n variable nodes, an edge interleaver, and $n - k$ check nodes. The ith variable node represents the ith bit of the code word. Suppose that this bit is involved in $d_{v,i}$ parity checks so that its node has $d_{v,i}$ edges going into the edge

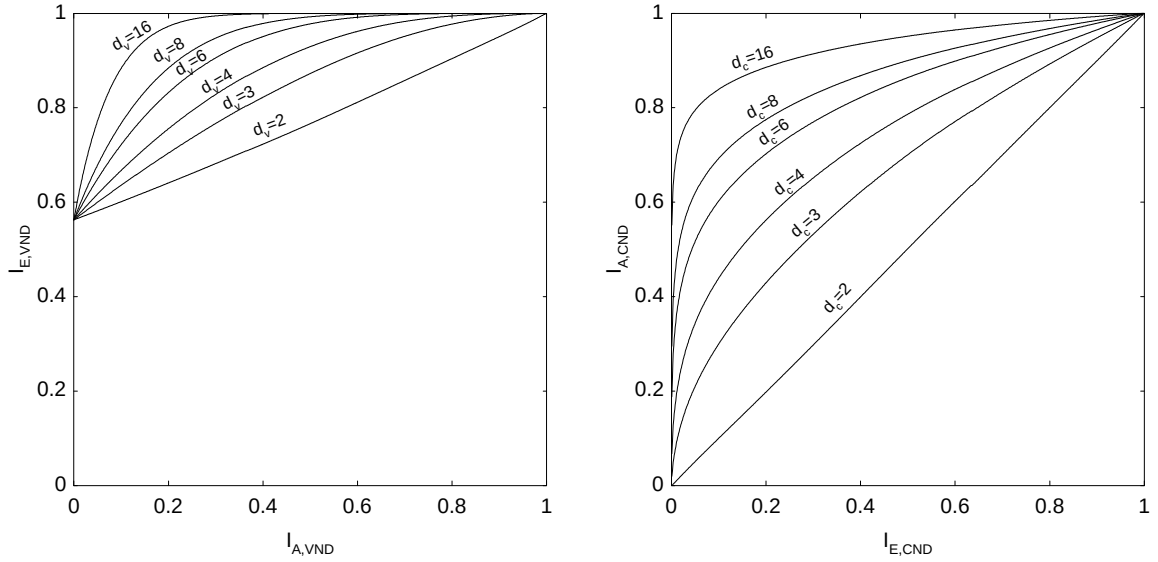

Fig. 1. Variable and check node decoder EXIT curves. The channel is the AWGN channel with $E_b/N_0 = 1$dB at a code rate of $R = 1/2$. Note the swapping of the *a priori* and extrinsic axes.

interleaver. The edge interleaver connects the variable nodes to the check nodes, each of which represents a parity–check equation. The ith check node checks $d_{c,i}$ bits so that it has $d_{c,i}$ edges. The sets of variable and check nodes are referred to as the variable node decoder (VND) and check node decoder (CND), respectively. Iterative decoding is performed by exchanging extrinsic information between the VND and CND.

We proceed by describing how to obtain EXIT curves for the VND and CND. We then discuss how to put these curves together to design good codes for the AWGN channel

A. EXIT Curve of the Inner Variable Node Decoder

A variable node of degree d_v has $d_v + 1$ incoming messages, d_v from the edge interleaver and one from the channel. The variable node decodes by adding log–likelihood ratio values (L–values [24]). More precisely, we have

$$L_{i,out} = L_{ch} + \sum_{j \neq i} L_{j,in} \tag{1}$$

where $L_{j,in}$ and $L_{j,out}$ are the jth extrinsic L–values going into and coming out of the variable node, respectively, and L_{ch} is the L–value coming from the channel. Consider the AWGN channel with binary antipodal (± 1) modulation and signal–to–noise ratio E_b/N_0. We assume that the $L_{j,in}$ are Gaussian distributed. The EXIT function of a degree–d_v variable node is then

$$I_{E,VND}\left(I_A, d_v, E_b/N_0\right) = J\left(\sqrt{(d_v - 1)\left[J^{-1}\left(I_A\right)\right]^2 + \sigma_{ch}^2}\right) \tag{2}$$

where the $J(\cdot)$–function is given in the Appendix and $\sigma_{ch}^2 = 8R \cdot E_b/N_0$. Fig. 1 (left) plots several variable node curves when $R = 1/2$ and $E_b/N_0 = 1$dB. Observe that $I_{E,VND}(0, d_v, E_b/N_0)$ is the capacity of the channel at the E_b/N_0 that is being considered.

B. EXIT Curve of the Outer Check Node Decoder

The decoding of a degree d_c check node corresponds to the decoding of a length d_c (or rate $(d_c - 1)/d_c$) single parity check code. The output L–values are thus (see [24,

Sec. II.A])

$$L_{i,out} = \ln \frac{1 - \prod_{j \neq i} \frac{1-e^{L_{j,in}}}{1+e^{L_{j,in}}}}{1 + \prod_{j \neq i} \frac{1-e^{L_{j,in}}}{1+e^{L_{j,in}}}}. \tag{3}$$

For code design we will later assume that the $L_{j,in}$ (but not the $L_{i,out}$) are Gaussian distributed. We point out that for numerical stability it is better to compute (3) recursively in the logarithmic domain rather than directly.

The check node EXIT curves can be computed by simulation. Alternatively, for the binary erasure channel a duality property exists [25] that gives the EXIT curve $I_{E,SPC}(\cdot)$ of the length d_c single parity check code in terms of the EXIT curve $I_{E,REP}(\cdot)$ of the length d_c (or rate $1/d_c$) repeat code, i.e.,

$$I_{E,SPC}(I_A) = 1 - I_{E,REP}\left(1 - I_A\right). \tag{4}$$

Simulations show that this property is in fact an accurate approximation for Gaussian *a priori* inputs. We thus approximate the check node EXIT curves as

$$I_{E,CND}(I_A) \approx 1 - I_{E,REP}\left(1 - I_A\right) = 1 - J\left(\sqrt{d_c - 1} \cdot J^{-1}\left(1 - I_A\right)\right) \tag{5}$$

where the second step follows by using (2) with $\sigma_{ch}^2 = 0$. It is further useful to express (5) in terms of its inverse function, i.e.,

$$I_{A,CND}(I_E) \approx 1 - J\left(\frac{J^{-1}\left(1 - I_E\right)}{\sqrt{d_c - 1}}\right). \tag{6}$$

Fig. 1 (right) plots several check node curves. Observe that the curves are similar to the VND curves except that they all start from the origin.

C. Code Design by Curve Fitting

We will consider only *check–regular* LDPC codes, i.e., all check nodes have degree d_c (in [26] these are called *right–regular* codes). The remaining LDPC design involves specifying the variable node degrees $d_{v,i}$, $i = 1, \ldots, n$. Let D be the number of different variable node degrees, and denote these degrees by $\widetilde{d}_{v,i}$, $i = 1, \ldots, D$. The average variable node degree is

$$\overline{d}_v = \sum_{i=1}^{D} a_i \cdot \widetilde{d}_{v,i} \tag{7}$$

where a_i is the fraction of *nodes* having degree $\widetilde{d}_{v,i}$. Note that the a_i must satisfy $\sum_i a_i = 1$. Since the number of edges at the VND and CND are the same, we have $n\,\overline{d}_v = (n-k)\,d_c$ or

$$\overline{d}_v = (1 - R) \cdot d_c. \tag{8}$$

Let b_i be the fraction of *edges* involved with variable nodes having degree $\widetilde{d}_{v,i}$. There are in total $(n\,a_i)\,\widetilde{d}_{v,i}$ edges involved with such nodes, so we have

$$b_i = \frac{n\,a_i\,\widetilde{d}_{v,i}}{n\,\overline{d}_v} = \frac{\widetilde{d}_{v,i}}{(1 - R)\,d_c} \cdot a_i. \tag{9}$$

Note that the b_i must satisfy $\sum_i b_i = 1$. In [25], [27] it is shown that the EXIT curve of a mixture of codes is an average of the component EXIT curves. We must here average using the b_i (and not the a_i) because it is the *edges* that carry the extrinsic messages. The effective VND transfer curve is thus given by

$$I_{E,VND}\left(I_A\right) = \sum_{i=1}^{D} b_i \cdot I_{E,VND}\left(I_A, \widetilde{d}_{v,i}\right) \tag{10}$$

i.e., (10) is a weighted sum of the curves of on the left in Fig. 1. Note that only $D-2$ edge fractions can be adjusted because we must enforce (8) and $\sum_i b_i = 1$. Thus, in order to have any flexibility we must choose $D \geq 3$. We shall see that $D = 3$ already gives surprisingly good results.

D. Design Example

In [25] (see also [27]) it is shown that to approach capacity on binary erasure channels one must match the VND and CND transfer curves. Experience shows that the same is true for other channels. To match the curves we note that $I_{E,VND}(0)$ is the channel capacity for a specified E_b/N_0. We design codes with $R = 1/2$, and choose $E_b/N_0 = 0.5$dB so that $I_{E,VND}(0) \approx 0.524$ is slightly larger than R. We further choose d_c so that the CND transfer curve has a reasonable distance from the y–axis at $I_{A,CND} = 1/2$. This approach simplifies finding a VND curve with $I_{E,VND}(0) \approx 0.524$ that lies above the CND curve. Furthermore, this gives the decoder a good "head start" at the first iteration.

For simplicity we restrict the VND to have only three different variable node degrees ($D = 3$). This means that only one b_i can be chosen freely, and Fig. 2 shows a manual curve fit whose variable node parameters are as follows:

$$\begin{array}{lll} \widetilde{d}_{v,1} = 2, & a_1 = 0.508, & b_1 = 0.254, \\ \widetilde{d}_{v,2} = 4, & a_2 = 0.419, & b_2 = 0.419, \\ \widetilde{d}_{v,3} = 18, & a_3 = 0.073, & b_3 = 0.327. \end{array}$$

For this simple example we obtain a convergence threshold of about 0.5dB while the capacity is at 0.19dB (see also [5]). A simulation with $n = 10^5$, a random edge interleaver, and 60 iterations shows a turbo cliff at about 0.55dB (we measure the turbo cliff at a bit error rate (BER) of 10^{-5}). After 200 iterations the turbo cliff is at 0.5dB, which demonstrates the accuracy of the EXIT chart and our approximations.

We remark that by choosing a larger D and using sophisticated curve fits one can match the VND curve more closely to the CND curve. One can also model the *a priori* knowledge more carefully than as Gaussian random variables. However, any improvement over the approach outlined above will only be marginal.

III. MIMO Detection and LDPC Decoding

We next turn to multi–antenna modulation and detection (see Fig. 3). Suppose there are M transmit and N receive antennas. Each transmitter symbol is thus an $M \times 1$ vector $\mathbf{s} = [s_1, ..., s_M]^T$ whose entries take on complex values in a constellation set. We consider constellations of size 2^{M_c} so that each symbol carries $M \cdot M_c$ coded bits. For example, for quadrature phase–shift keying (QPSK) we have $M_c = 2$ and for 16 quadrature amplitude modulation (16–QAM) we have $M_c = 4$. The average energy per transmit symbol is limited to E_s, and we further assume that $E[||s_m||^2] = E_s/M$.

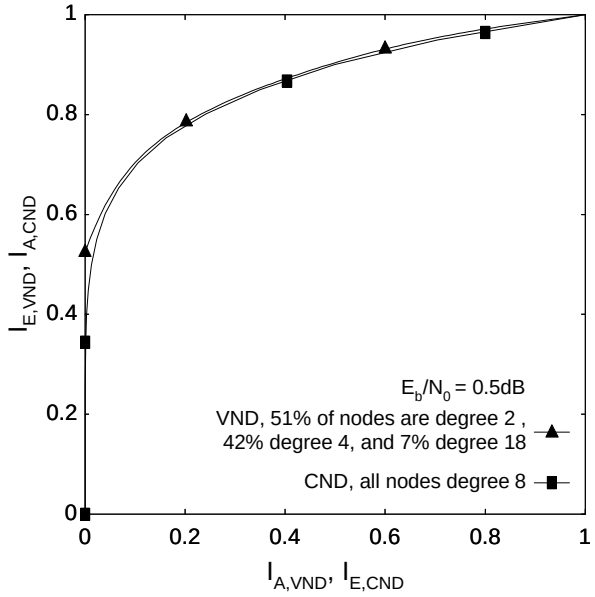

Fig. 2. Design example of a check–regular LDPC code with $R = 1/2$ at $E_b/N_0 = 0.5$dB. The VND curve is a mixture of the variable node degrees $\widetilde{d}_{v,1} = 2$, $\widetilde{d}_{v,2} = 4$ and $\widetilde{d}_{v,3} = 18$.

The receiver sees vectors $\mathbf{y} = \mathbf{H}\mathbf{s} + \mathbf{n}$ of size $N \times 1$, where $\mathbf{H}$ is the $N \times M$ channel matrix and $\mathbf{n}$ is a $N \times 1$ noise vector. We assume $\mathbf{H}$ to be known by the receiver only, and the entries of $\mathbf{n}$ to be independent, complex, zero–mean, Gaussian random variables with variance $\sigma^2 = N_0/2$ per real component. We define the normalized signal–to–noise ratio E_b/N_0 as

$$\left.\frac{E_b}{N_0}\right|_{\text{dB}} = \left.\frac{E_s}{N_0}\right|_{\text{dB}} + 10\log_{10}\frac{N}{RMM_c}. \tag{11}$$

The MIMO detector performs *a posteriori* probability (APP) bit detection by considering all 2^{MM_c} possible hypotheses on $\mathbf{s}$ [15]–[19]. Alternatively, one might consider only a subset of hypotheses by using list sphere detection (LSD) [19]. The detector's soft output is forwarded to the decoder, which in turn computes extrinsic information to be used as *a priori* knowledge by the detector for the next iteration. This is in analogy to iterative decoding of serially concatenated codes [28].

Suppose we encounter Rayleigh fading so that the entries of $\mathbf{H}$ are independent, complex, zero–mean, Gaussian random variables with unit variance [8, Sec. 4]. For a *piecewise constant* channel the matrix $\mathbf{H}$ remains unchanged over long time intervals, while for an *ergodic* channel $\mathbf{H}$ changes for every symbol $\mathbf{s}$. We consider only the ergodic model whose capacity is (see [7], [8])

$$C = E\left[\log_2 \det\left(\mathbf{I}_N + \frac{E_s}{N_0}\frac{1}{M}\mathbf{H}\mathbf{H}^\dagger\right)\right] \tag{12}$$

where $\mathbf{H}^\dagger$ denotes the complex–conjugate transpose of $\mathbf{H}$. One achieves capacity by using Gaussian distributed symbols $\mathbf{s}$. However, in practice the entries of $\mathbf{s}$ are constrained to come from QAM constellations.

We proceed by showing how to compute EXIT curves for the MIMO detector. We then describe a combined demodulation/decoding structure that is flexible enough to approach MIMO capacity. The structure automatically specifies how the encoding/modulation is done. Finally, we show how to match the resulting two EXIT curves.

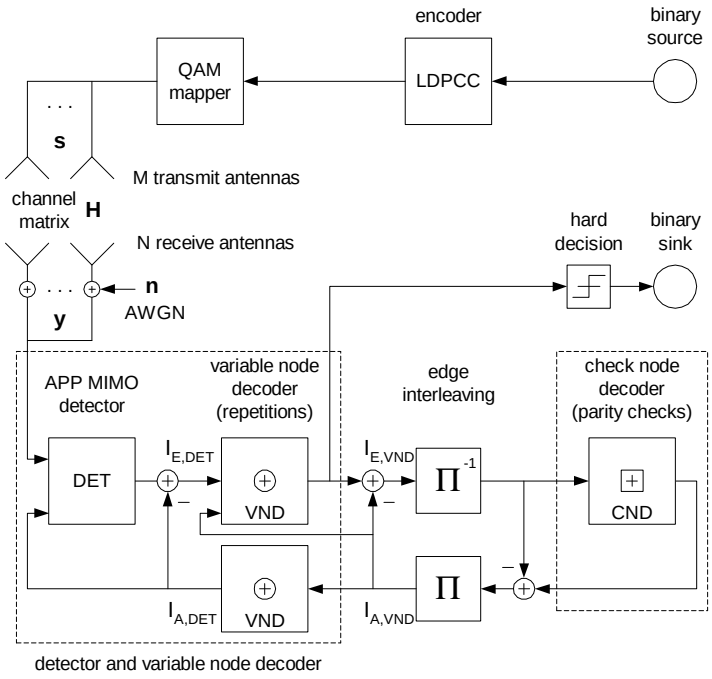

Fig. 3. The MIMO model. The receiver has a MIMO detector, variable node decoders and a check node decoder.

A. EXIT Curve of the MIMO Detector

The MIMO detector accepts *a priori* L–values and computes *a posteriori* L–values that are converted to extrinsic messages before being forwarded to the VND. The detector EXIT curve cannot be described in closed form but one can accurately estimate it by Monte–Carlo simulation [10]. We denote the curve by

$$I_{E,DET}\left(I_{A,DET}, E_b/N_0\right). \tag{13}$$

Fig. 4 shows simulated EXIT curves of MIMO detectors for different numbers of transmit and receive antennas. The modulation used is Gray–mapped QPSK. Observe that most of the curves resemble straight lines. The 1×1–curve is provided as a reference.

B. EXIT Curve of the Combined MIMO Detector and Variable Node Decoder

We combine the MIMO detector and the LDPC variable node decoder as shown in Fig. 3. The detector consists of $n/(MM_c)$ individual detectors (or detector nodes) that are each connected to MM_c variable nodes. Consider the three boxes in Fig. 3 corresponding to one of these individual detector/VNDs. For simplicity, we denote the EXIT curve of this structure by $I_{E,VND}(\cdot)$ and assume that the *a priori* L–values are Gaussian distributed. We further choose all the MM_c variable nodes to have the same degree d_v. Thus, using (2) we find that the lower VND in Fig. 3 maps $I_{A,VND}$ into

$$I_{A,DET} = J\left(\sqrt{d_v} \cdot J^{-1}\left(I_{A,VND}\right)\right). \tag{14}$$

Next, we *separately* measure the transfer curve (13) by Monte–Carlo simulation for a given E_b/N_0. The advantage of considering the MIMO detector and the lower VND separately is that E_b/N_0 affects only (13) and not (14). We approximate the measured

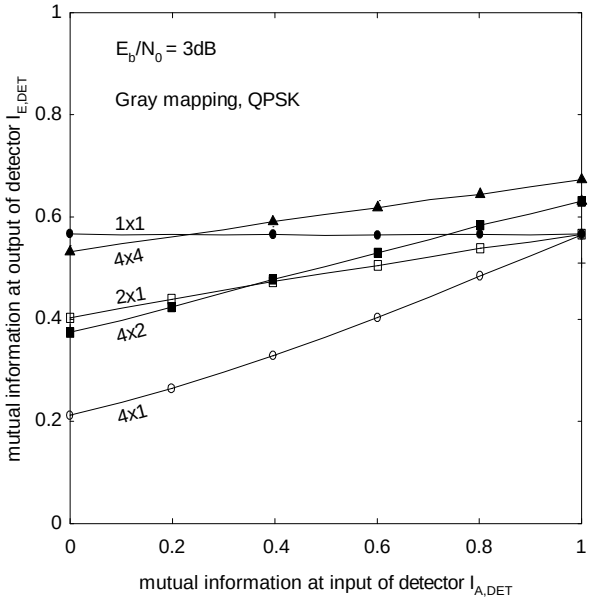

Fig. 4. $M \times N$ MIMO detector transfer curves at $E_b/N_0 = 3$dB assuming a code rate of $R = 1/2$. The constellation set is QPSK.

$I_{E,DET}\left(I_{A,DET}, E_b/N_0\right)$ curves (13) by 3rd order polynomials. For example, our approximation for the 4×1 MIMO detector with QPSK at $E_b/N_0 = 7$dB is

$$I_{E,DET}\left(I_{A,DET}, E_b/N_0 = 7\text{dB}\right) = -0.171 \cdot I_{A,DET}^3 + 0.271 \cdot I_{A,DET}^2 + 0.393 \cdot I_{A,DET} + 0.269. \quad (15)$$

This will let us express the combined detector/VND EXIT curve in closed form, which is convenient for curve fitting.

The third step is to consider the upper VND in Fig. 3. We approximate the EXIT curve of the combined MIMO detector and VND as

$$I_{E,VND}\left(I_{A,VND}, I_{E,DET}, d_v\right) = J\left(\sqrt{(d_v - 1) \cdot \left[J^{-1}\left(I_{A,VND}\right)\right]^2 + \left[J^{-1}\left(I_{E,DET}\right)\right]^2}\right), \quad (16)$$

where we have used (2) with

$$\sigma_{ch}^2 = \left[J^{-1}\left(I_{E,DET}\right)\right]^2 \quad (17)$$

Finally, inserting (13), (14), and a polynomial like (15) into (16) we obtain the desired transfer curve in the form

$$I_{E,VND}\left(I_{A,VND}, d_v, E_b/N_0\right). \quad (18)$$

Fig. 5 (left) shows some combined detector and VND transfer curves. Observe that the "pure" detector transfer curve of Fig. 4 is recovered by setting $d_v = 1$ in (18).

C. Design Examples

We design check–regular LDPC codes by matching the curve (18) to the CND curve. Again, we restrict ourselves to just three different variable node degrees ($D = 3$) so that the curve fit can be performed manually. This simple approach gives surprisingly

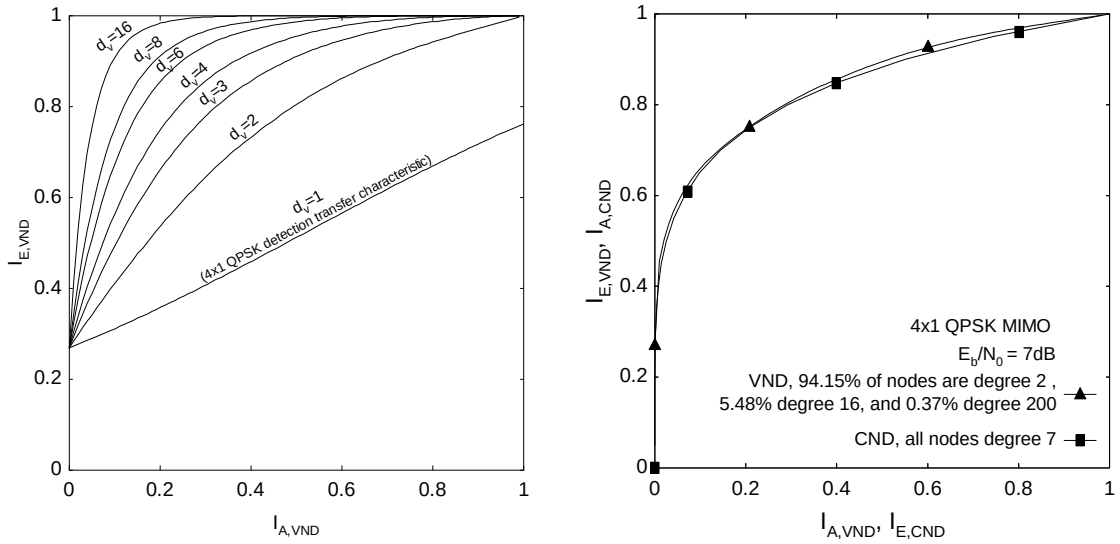

Fig. 5. (Left) Combined 4×1–detector and VND transfer curves at $E_b/N_0 = 7$dB and $R = 1/2$. (Right) Curve fit of the 4×1 LDPC modulation scheme at $E_b/N_0 = 7$dB. The code rate is $R = 1/2$.

TABLE I
CODE PARAMETERS FOR $M \times N$ MIMO USING QPSK

4×1			4×2		
Capacity E_b/N_0 at 6.65dB			Capacity E_b/N_0 at 2.95dB		
Curve fit at 7.00dB			Curve fit at 3.30dB		
BER 10^{-5} at 7.90dB			BER 10^{-5} at 3.60dB		
$d_c = 7$			$d_c = 6$		
$\widetilde{d}_{v,i}$	a_i [%]	b_i [%]	$\widetilde{d}_{v,i}$	a_i [%]	b_i [%]
2	94.15	53.80	2	69.78	46.52
16	5.48	25.05	3	26.12	26.12
200	0.37	21.15	20	4.10	27.36

powerful coded modulation schemes. Table I shows the parameters of our curve fitting for the 4×1 and 4×2 MIMO channels. Fig. 5 (right) plots the corresponding EXIT chart for a 4×1 MIMO channel.

Fig. 6 shows simulation results with QPSK, $R = 1/2$, $n = 10^5$, a random edge interleaver, and 60 iterations. Our approach turns out to be quite successful: All LDPC modulation schemes operate within about 1dB of their respective capacity limits (see Table I). We remark again that the gaps to capacity in Fig. 6 (or Table I) can be narrowed further by using $D > 3$ and better curve fits. The performance curves of a MIMO bit-interleaved coded modulation employing a UMTS standard turbo code with memory 3 constituent codes are given as references. Note that the turbo code does not interact efficiently with the MIMO detector when $M > N$, as was already pointed out in [10]. It turns out that more detector/internal decoder iterations hardly improve the bit error rate.

D. Comparison with Space–Time Block Codes

Consider the 2×1 MIMO channel with QPSK and a rate 1/2 LDPC code. The spectral efficiency is 2 bits per channel use. Suppose next that we use a space–time block code as an inner code [20]. This scheme obtains a diversity gain with what is in effect a rate

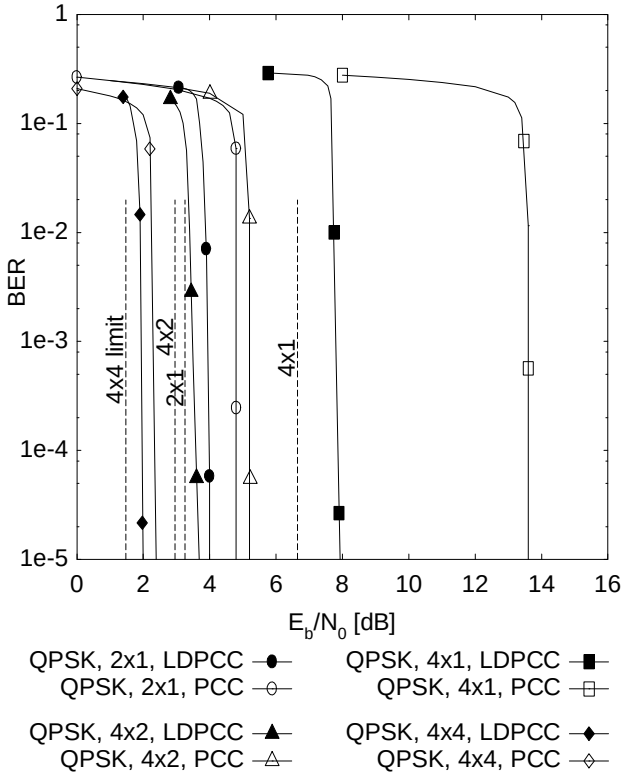

Fig. 6. Bit error rates for combined MIMO detection/decoding with QPSK on a Rayleigh fading channel. All codes have $n = 10^5$ and $R = 1/2$ for a total rate of M bits per channel use. LDPC codes: 60 iterations. Parallel concatenated (turbo) code: UMTS standard, memory 3, with 4 detector/decoder iterations and 20 internal decoder iterations each.

1/2 repeat code. Thus, to achieve 2 bits per channel use with a rate 1/2 outer code one must compensate for the inner code rate loss by changing the constellation from QPSK to 16–QAM. But 16–QAM complicates the detection and requires a power amplifier that is linear over a wide range. These issues will be even more pronounced for 4×1 MIMO channels. For example, the scheme proposed here achieves a spectral efficiency of 4 bits per channel use with QPSK modulation and a rate 1/2 LDPC code. A corresponding space–time block code [21], which is in effect a rate 1/4 repeat code, would have to use 256–QAM to achieve 4 bits per channel use with a rate 1/2 outer code. This is not practical in a wireless system. Furthermore, no orthogonal space–time block code exists for the 4×1 MIMO channel [21] which makes this approach even less attractive.

Appendix: The $J(\cdot)$–Function

The $J(\cdot)$–function is the mutual information between a binary random variable x with $\Pr(x = \mu) = \Pr(x = -\mu) = 1/2$ and $y = x + n$ where n is a zero–mean, Gaussian random variable with variance σ^2. We consider y as an L–value based on Gaussian distributions, and set $\mu = \sigma^2/2$ to fulfill a symmetry condition (see, e.g., [29]). We have

$$J(\sigma) = H(x) - H(x|y) = 1 - \int_{-\infty}^{\infty} \frac{e^{-\frac{\left(\xi - \sigma^2/2\right)^2}{2\sigma^2}}}{\sqrt{2\pi\sigma^2}} \cdot \log_2\left[1 + e^{-\xi}\right] \, d\xi \tag{19}$$

where $H(x)$ is the entropy of x and $H(x|y)$ is the entropy of x conditioned on y. We can use $J(\cdot)$ to compute the capacity of a binary input/continuous output AWGN channel with $x \in \{\pm 1\}$ and zero–mean noise with variance σ_n^2. The capacity is $J(2/\sigma_n)$.

References

[1] R. G. Gallager, "Low–Density Parity–Check Codes," Sc.D. thesis, Mass. Inst. Tech., Cambridge USA, Sept. 1960.

[2] R. G. Gallager, "Low–density parity–check codes," *IEEE Trans. Inform. Theory*, vol. 8, pp. 21–28, Jan. 1962.

[3] M. G. Luby, M. Mitzenmacher, M. A. Shokrollahi, D. A. Spielman, " Efficient erasure correcting codes," *IEEE Trans. Inform. Theory*, vol. 47, no. 2, pp. 569–584, Feb. 2001.

[4] T. J. Richardson, R. L. Urbanke, "The capacity of low–density parity–check codes under message–passing decoding," *IEEE Trans. Inform. Theory*, vol. 47, no. 2, pp. 599–618, Feb. 2001.

[5] S. Y. Chung, G. D. Forney, T. J. Richardson, R. Urbanke, "On the design of low–density parity–check codes within 0.0045dB of the Shannon limit," *IEEE Comm. Lett.*, vol. 5, no. 2, pp. 58–60, Feb. 2001.

[6] S. ten Brink, "Convergence of iterative decoding," *Electron. Lett.*, vol. 35, no. 10, pp. 806–808, May 1999.

[7] G. J. Foschini, "Layered space–time architecture for wireless communication in a fading environment when using multi–element antennas," *Bell Labs. Tech. J.*, vol. 1, no. 2, pp. 41–59, 1996.

[8] I. E. Telatar, "Capacity of multi–antenna Gaussian channels," *Eur. Trans. Telecom.*, vol. 10, pp. 585–595, Nov. 1999.

[9] E. Biglieri, J. Proakis, S. Shamai (Shitz), "Fading channels: information-theoretic and communications aspects" *IEEE Trans. Inform. Theory*, vol. 44, no. 2, pp. 2619–2692, Oct. 1998.

[10] S. ten Brink, B. M. Hochwald, "Detection thresholds of iterative MIMO processing," *Proc. Int. Symp. Inform. Theory*, July 2002.

[11] B. Lu, X. Wang, K. Narayanan, "LDPC–based space–time coded OFDM systems over correlated fading channels: performance analysis and receiver design," *IEEE Trans. Commun.*, vol. 50, pp. 74–88, Jan. 2002.

[12] G. Ungerboeck, "Channel coding with multilevel/phase signals," *IEEE Trans. Inform. Theory*, vol. 28, no. 1, pp. 55–67, Jan. 1982.

[13] G. Caire, G. Taricco, E. Biglieri, "Bit-interleaved coded modulation," *IEEE Trans. Inform. Theory*, vol. 44, no. 3, pp. 927–946, May 1998.

[14] C. Berrou, A. Glavieux, P. Thitimajshima, "Near Shannon limit error–correcting coding and decoding: Turbo–codes," *Proc. ICC*, pp. 1064–1070, May 1993.

[15] A. M. Tonello, "Space–time bit–interleaved coded modulation with an iterative decoding strategy," *Proc. VTC*, pp. 473–478, Sept. 2000.

[16] A. van Zelst, R. van Nee, G. Awater, "Turbo–BLAST and its performance," *Proc. VTC*, May 2001.

[17] A. Stefanov and T. Duman, "Turbo–coded modulation for systems with transmit and receive antenna diversity over block fading channels: system model, decoding approaches, and practical considerations," *IEEE J. Sel. Areas Comm.*, vol. 19, pp. 958–968, May 2001.

[18] C. Schlegel and A. Grant, "Concatenated space–time coding," *Proc. PIMRC*, San Diego, CA, Sept. 2001.

[19] B. M. Hochwald, S. ten Brink, "Iterative List Sphere Decoding to Attain Capacity on a Multi–Antenna Link," *39th Ann. Allerton Conf. on Commun., Control, and Computing*, October 2001.

[20] S. M. Alamouti, "A simple transmit diversity technique for wireless communications," *IEEE Journ. on Select. Areas in Commun.*, vol. 16, pp. 1451–1458, Oct. 1998.

[21] V. Tarokh, H. Jafarkani and A. R. Calderbank, "Space–time block codes from orthogonal designs," *IEEE Trans. Inform. Theory*, vol. 45, pp. 1456–1467, July 1999.

[22] D. Divsalar, S. Dolinar, F. Pollara, "Low complexity turbo–like codes", *Proc. 2nd Int. Symp. on Turbo Codes*, pp. 73–80, Sept. 2000.

[23] H. El Gamal, A. R. Hammons, Jr., "Analyzing the turbo decoder using the Gaussian approximation," *IEEE Trans. Inform. Theory*, vol. 47, no. 2, pp. 671–686, Feb. 2001.

[24] J. Hagenauer, E. Offer, L. Papke, "Iterative decoding of binary block and convolutional codes," *IEEE Trans. Inform. Theory*, vol. 42, no. 2, pp. 429–445, Mar. 1996.

[25] A. Ashikhmin, G. Kramer, S. ten Brink, "Extrinsic information transfer functions: A model and two properties," *36th Ann. Conf. on Inf. Sci. and Syst.*, Princeton, Mar. 2002.

[26] M. A. Shokrollahi, "New sequences of linear time erasure codes approaching the channel capacity," *Proc. 13th Conf. Applied Algebra, Error Correcting Codes, and Cryptography (Lecture Notes in Computer Science)*, Springer Verlag, Berlin Germany, 1999, pp. 65–76.

[27] M. Tuechler, J. Hagenauer, "EXIT charts and irregular codes," *36th Ann. Conf. on Inf. Sci. and Syst.*, Princeton, Mar. 2002.

[28] S. Benedetto, D. Divsalar, G. Montorsi, F. Pollara, "Serial Concatenation of Interleaved Codes: Performance Analysis, Design, and Iterative Decoding," *IEEE Trans. Inform. Theory*, vol. 44, no. 3, pp. 909–926, May 1998.

[29] P. Hoeher, U. Sorger, I. Land, "Log–likelihood values and Monte Carlo simulation — some fundamental results," in *Proc. Int. Symp. on Turbo Codes & Related Topics*, pp. 43–46, 2000.

[30] W. H. Press, S. A. Teukolsky, W. T. Vetterling, B. P. Flannery, *Numerical Recipes in C*, Cambridge University Press, New York, 1997.